CONTROLLED DISTRIBUTION OF COMPOSITION WITHIN EXTRUSIONS AS ENABLED BY AN ACTIVE-MIXING HOTEND

I. A. Rybak*, D. L. Hernandez†, R. V. Gonzalez*, and J. T. Green*

*Department of Engineering Education and Leadership, The University of Texas at El Paso, El Paso, TX, 79968

†Department of Aerospace and Mechanical Engineering, The University of Texas at El Paso, El Paso, TX, 79968

Abstract

Local control of composition in additive manufacturing has great potential for improving properties and multifunctional characteristics of printed materials. Dimensional resolution of such composition control in fused filament fabrication is usually limited to the geometry of a single extrusion. To achieve microstructural control within extrusions, an active-mixing hotend was configured to extrude with various proportions of mixing rod rotation and material flow. Distribution control was investigated through optical characterization of extrusion cross-sections at steady state using various polymers, colors, and composites. When at low proportions relative to extrusion, rod rotation affects material phase shape and location. Resultant phase distributions are specific to the extruded material combinations and are affected by extrusion heights and widths. These mechanisms for controlling microstructures can be controlled *in situ* through software enabling fabrication of multifunctional materials with a wide variety of strength, stiffness, thermal and electrical conductivity, solubility, corrosion resistance, and more.

Keywords: Local Composition Control, Fused Filament Fabrication, Surface Coatings, Microstructure, Functional Gradients, Polymer Blends, Composites

Introduction

Additive manufacturing (AM) is favored across many industries and continues to be a major research topic. This is largely due to the intricate processes and toolchains of AM which enable production of materials with advanced properties and complex features. One important characteristic of such processes is the scale of the features which can be produced. Fused filament fabrication (FFF) is an AM technique having widespread integration into a variety of industries. This method utilizes thermoplastic filaments and operates at relatively low costs. Advancements in FFF continue to increase versatility ensuring its continued relevance as a focus of research. Notably the resolution and capabilities of composition control have greatly increased in recent work. In conventional processes, the print is uniform in composition, and the composition throughout the printed structure is determined by selecting an input filament. Some systems can switch between filaments or toolheads while printing to achieve a multi-material structure. Others can vary feed rates of multiple filaments into a single nozzle, but the filaments coextrude and do not distribute well throughout the extrusion. Conventionally, features in an FFF printed structure are geometrically limited to the size of the nozzle. If greater detail is desired, then a smaller nozzle may be necessary [1]. This increase in resolution usually increases print times since the smaller

nozzle restricts flow through the hotend and requires more length of toolpaths to achieve the same volume of output. Some systems use multiple toolheads with different nozzle diameters to achieve this increase in resolution without requiring a commensurate increase in print time.

Through use of an active-mixing hotend, shown in Figure 1A, *in situ* variations in composition control have been achieved including dynamic control throughout the print geometry providing effectively homogenous composition output, a capability known as local composition control (LCC). This was demonstrated by Green et al. to form a variety of gradients and polymer mixtures [2] as well as gradients of fiber volume fraction in composite structures [3]. In effect, an active-mixing hotend enables extrusion-scale composition control. Also demonstrated in Figure 1B, the mixing hotend can be used as a conventional system by only using one filament inlet at a time to achieve different scales of LCC. Extrusion-level composition control allows for a high range of composition control at a small print scale. Illustrations of composition control at different scales are provided in Figure 1C. Control of the balance between the flow of material into the hotend and the rotation of the mixing rod is achieved through the mixing feature of Marlin firmware (marlinfw.org) [4] with the active-mixing motor configured as an extruder motor. This allows for print instructions to include commands to set the input ratio of each extruder motor and scaling of the overall filament flow rate to counteract the loss of motor steps to the mixing motor rather than the three filament extrusions. In Figure 1D an equal blend of white, orange, and blue pigmented polylactic acid (PLA) filaments was achieved using the command "M165 A1 B1 C1" with the additional D parameter controlling the mixing motor. Because the weights of each extruder are normalized by the firmware, a rod rotation ratio of 1:1 [rod:filament] is achieved with the full command "M165 A1 B1 C1 D3" such that the ratio of steps sent to the rod's motor relative to the total steps sent to filament extruder motors is equal to 1. This causes the rod to spin 2.10 revolutions for every total millimeter of filament extruded.

Composition control can enable numerous features that are known to benefit material properties and performance for numerous applications. Material surfaces and interfaces have high impact on the end use of an additively manufactured structure, such as improving corrosion resistance and surface finishes but may require post processing techniques including chemical treatment or machining to achieve the desired properties [5–10]. Lahaie et al. demonstrated simultaneous increases in strength between layers alongside decreased warping by using acrylonitrile butadiene styrene (ABS) at interfaces with a polycarbonate core, resulting in increased impact strength [11]. This required the use of custom extrusion dies to create filaments with a static core and shell structure and fixed mixing proportions before printing, leading to increased impact strength. Active mixing of materials during fabrication allows for blends of materials with different tensile characteristics [12] as well as functionally graded structures intended to mimic biomechanical gradients [13]. LCC techniques allow for higher resolution of these structures through selective deposition *in situ* [14]. Multifunctional materials are a focus of research since they can fulfill multiple roles with fewer production processes, though the printing procedures can impact functionality [15,16]. Functionally graded materials are known to have many advantages that arise out of transitions between material properties including porosity, hardness, chemical and temperatures resistance, and composite additives [17,18]. In conjunction with multifunctional materials, functional gradients enable new applications such as damage detection and structural batteries [14,19,20]. Advancements in the scale and range of LCC capabilities can be applied to the exploration of these use cases and their importance in industry.

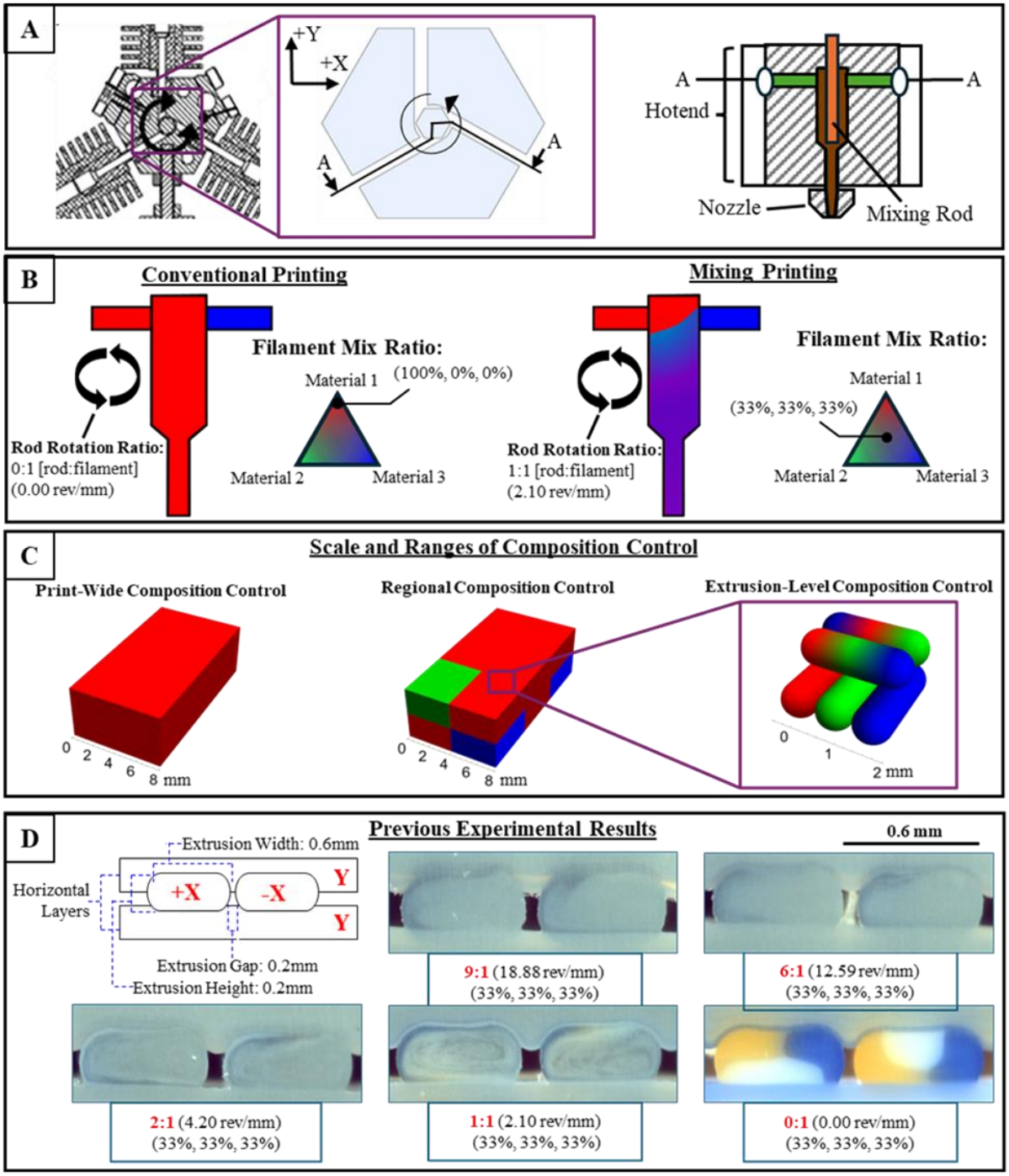

Figure 1 – Previous design work to achieve homogonous mixing in extrusions using an active-mixing hotend. A) Hotend design and section view of inlets utilized in this study relative to the print axes. B) Example types of composition control facilitated through print settings C) Local composition control applied at various scales including uniform composition assignment throughout a whole print, within regions of a print, or through individual extrusions using the hotend. D) Previous experimental results with three filaments (white, blue, and orange PLA) fed at equal rates with high homogeneity when mixed with high rod rotation ratios and individual phases of input filaments at low rod rotation ratios.

This study seeks to further advance the resolution of composition control to include microstructural distributions of composition within an extrusion during FFF printing using an active-mixing hotend. In previous work, the mixing rod was rotated in large proportions relative to the volume of filament extruded such that the mixture of materials is well distributed. In contrast, this study uses low proportions of mixing rod rotation to modify the distribution of materials in a controlled fashion. This causes the surface of an extrusion to be partially coated by the constituent materials, with the goal being to selectively coat an entire extrusion. To this end, the following hypotheses were tested experimentally under steady flow conditions:

1. The ratio of rod rotation primarily affects the center point of coating regions by shifting the center point in the direction of rod spin proportionally to the increase of rotation.
2. The ratio of the coating material proportionally increases the width of the coating as the portion of the coating material increases.
3. Coating center point and width is more sensitive to variation of rod rotation and coating proportion than it is to variations in combinations of materials

Methods

Printer configuration

The active-mixing hotend design from Green et al. [2] was used in this study with identical software and hardware configuration. Though it has three inlets, only the front two were used. Filaments were fed into inlets based on their role in the test. The core extrusion material was always inserted from the left side, 30° from the -X axis. The coating material was inserted from the right side, 30° from the +X axis. The third inlet was plugged to prevent leaking or contamination from other materials. The active-mixing rod was configured to rotate in the +Z direction, i.e. counterclockwise rotation when viewed from above. Prints were performed in ambient air at room temperature, 23° C.

Material selection

Input filaments were selected with different colors for all tests to enable optical assessment of the distribution of materials within an extrusion. To characterize the influence of material ratios and mixing rod velocity, tests were performed with PLA-based filaments having different colors. By having a consistent base material, effects from variations in viscosity are minimized. PLA was chosen for its printability and previous success in the active-mixing hotend. Red PLA represented the primary structure of the extrusion and blue represented the material to control distribution within the extrusion.

To investigate the influence of material combinations on the center point and width of coatings, two filaments were used to coat a primary structure composted of clear PLA. One filament, PLA containing chopped carbon fibers (PLAwCF) from ProtoPasta, was selected to represent the effect of a combination of composites. The other filament, black pigmented polyethylene terephthalate glycol (PETG) from MatterHackers, was selected to represent the shifts in a coatings center and width which may be observed when blending different polymers. Similarity in process parameters relative to PLA was a high priority when selecting materials to

ensure compatibility during printing. Both filaments have a black appearance which visually separated them from the clear PLA which is transparent in appearance. To minimize contamination from PETG or carbon fibers, these tests were performed on a separate printer including test with colored PLA as a control.

Print design and specimen fabrication

Print commands were generated using custom software designed to fill a rectangular prism with linear extrusion paths oriented at 0° and 180° to the positive X axis of the printer on the second and fourth layer. Supporting and compressing layers above and below these extrusions had linear paths oriented at 90° and 270° to the positive X axis. Filament mix ratios and rod rotation ratios were prescribed at the beginning of the print code and the hotend was primed by the printer operator prior to running print code. Extrusion length was increased in print commands following the proportion of the prescribed rod rotation ratios as required to provide normal flow despite the fact that some motor steps which conventionally contribute to extrusion are instead used for mixing motor rotation. Print and travel speeds were set to 10 and 100 mm/s to replicate conditions commonly used for the active-mixing printers. Extrusion volumes and print coordinates were calculated to achieve the prescribed extrusion width and height as necessary to print the rectangular prism shape with gaps between extrusions set to 0.2 mm. Print parameters are detailed in Table 1.

Table 1 – Print properties for specimens measured in this study

	Printer	Rod Velocity	Ratio of Coating per Total Extrusion	Extrusion Width	Extrusion Height	Extrusion Gap	Nozzle diameter	Temperatures Nozzle/Bed	Speed Print/Travel
	A/B*	rev/mm	%	mm	mm	mm	mm	°C	mm/s
Variable Filament Ratios	A	0.84	0 - 90	0.4	0.4	0.2	0.40	220/60	10/100
Variable Rod Velocity	A	0.0-2.1	10	0.4	0.4	0.2	0.40	220/60	10/100
Variable Material	B	0.84	10	0.4	0.4	0.2	0.40	220/60	10/100
Variable Aspect Ratio	A	0.84	10	0.4	0.2, 0.4	0.2	0.40	220/60	10/100

Notes:
*Printers A and B are identical in design and construction. Printer A has never printed or processed composite materials. Printer B has previously printed composites and was used to keep printer A free from potential contaminants.

Print parameters were adjusted to produce extrusions with a round shape and intentionally large gaps between extrusion toolpaths. To minimize flow processes external to the nozzle and improve optical analysis of microstructures, gaps were intentionally included between extrusions. Unless otherwise noted, the extrusion width and height were instructed to be of equal length, 0.4 mm, set to match the diameter of the nozzle. This was done to produce round extrusion cross sections rather than the more common oval shapes that are used in FFF. Prints were sized to ensure that flow is steady at the middle of the prism where specimens are cross sectioned for measurement.

Cross-sectioning and optical characterization

Each specimen was sectioned with a blade and sanded to the middle of the length as illustrated in Figure 2. The surfaces of the cross-section were coarsely sanded and then sanded with finer grits until the extrusions were clearly visible and cleaned to remove debris from the sanding process. Images were collected of each cross section and analysis was performed on the 6 & 7th extrusions from the front of the print, which were printed in the negative and positive X directions respectively, to minimize deformation from the edge of the print. Unless otherwise noted, all measurements were collected from the 4th layer to reduce measurement error from bed defects on the extrusions. Lighting and color calibration was adjusted and fixed during specimen image capture to maintain consistency of appearance for coating measurements. In all situations, a single material in any combination was selected as the "coating material" that was to be measured, even if it was the prominently present material in the filament proportion. Angular measurements were performed using the tools in the imaging software by the same researcher to reduce human error in classification of coating surface boundaries.

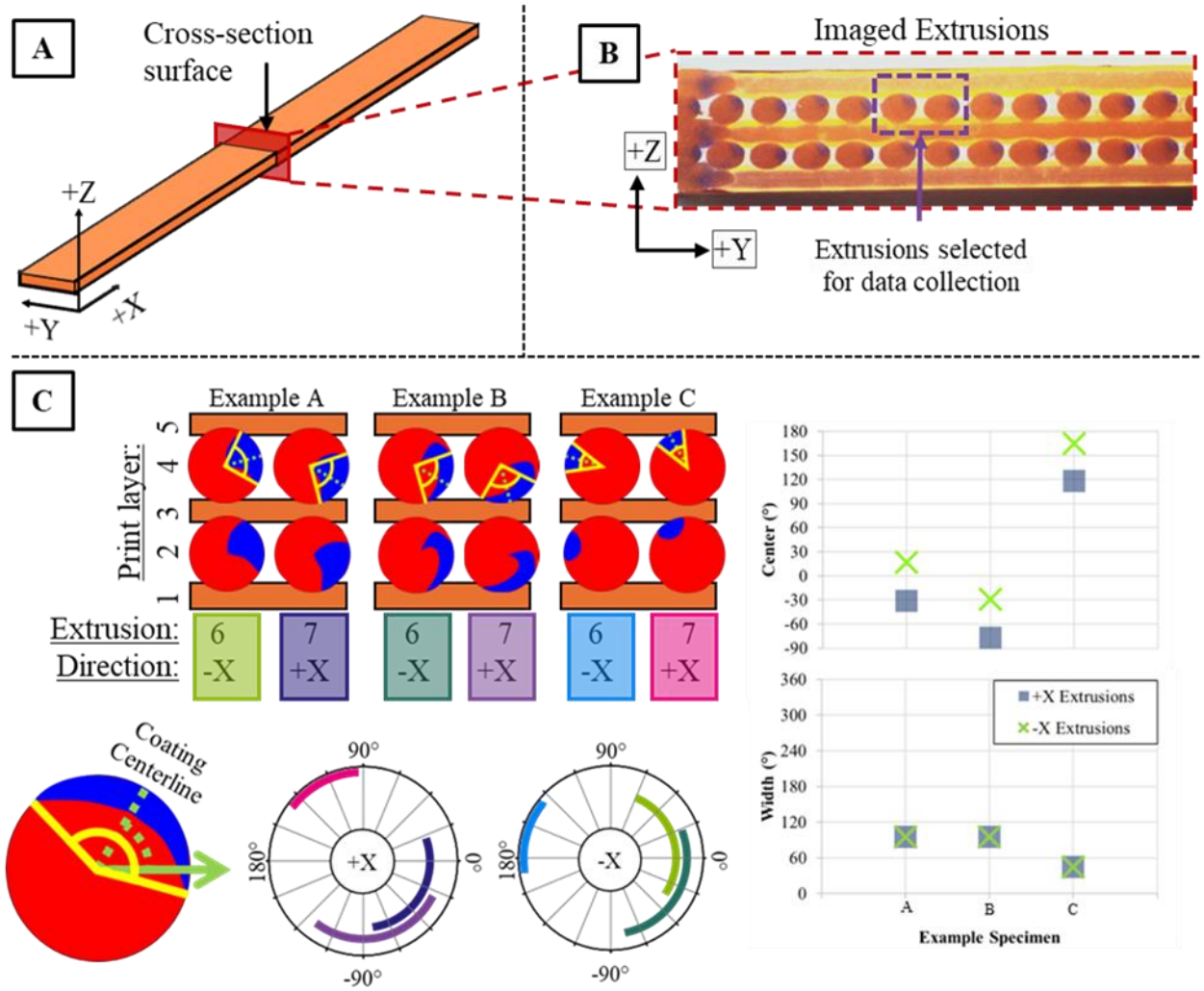

Figure 2 – Print design, cross-sectioning technique, optical measurement, and analysis methods. A. The print geometry is a rectangle with primary extrusions traveling in the + and – X direction for measurement. It is cut and sanded at the middle point to ensure steady state flow from the nozzle. B. Representative image of a surface image and the extrusions chosen for measurement. C. Example coating styles and the resultant measurements from the examples. While they do not represent experimental results, their readings demonstrate how specimens are analyzed in this study.

Analysis

Classification of composition in the extrusion was limited to the surface coatings and did not consider internal structure shape, size, or mixed regions Angular measurements were used to characterize a coating in terms of its angular width and the middle point between its ends, measured from a 0° reference. Some print configurations resulted in mixing at the interface between filaments, making a coating's boundaries less defined and more difficult to measure. For these situations, coating measurements selected the minimal region that best represented the coating material. In Figure 2, arbitrary, diagrammatic examples of these measurements are given to demonstrate how the data was collected and defined. Examples A and B demonstrate how coatings with different internal structures may result in the same representative values as the surface of each extrusion has the same width and falls at the same location. Example C presents an extrusion which has a much smaller coating size and a different position on the extrusion.

Results

Specimen Analysis

From measuring multiple extrusions in a single print with a 10% coating mixed at 0.84 rev/mm, shown in Figure 3, the center point and widths of extrusions varied by the values shown in Table 2. For this analysis, 20 extrusions were measured, 5 in each print direction for each measurable layer of the specimen. The standard deviation (SD) of width and center point for each direction is calculated using Eq. 1

$$SD = \sqrt{\frac{\sum(d-u)^2}{(n-1)}} \quad \text{(Eq. 1)}$$

where d is the data point's width or height, u is the average value for the set of n data points. The average deviation within a layer and the deviation between identical extrusions through the whole print are also presented. It is observed that on average, extrusions appear similar both within a layer and through the whole print. These small deviations indicate repeatability of coating deposition under similar conditions. All further specimens in this study limited data collection to extrusions 6 and 7 of the 4th layer. This repeatability print, and all prints analyzed in this study are presented in Figure 4. The red and blue pigment in the colored PLA specimens appears to blend more than using the clear and black materials when changing materials. Additionally, the dominance of the blue pigment over the red likely causes a perceived increase in the size of the coating and its resulting measurement and does not necessarily reflect the actual composition of the coating [14]. The specimens with PLAwCF and PETG coatings appear visually different because of optical transparency, allowing for additional depth in coloration. The potential impact of this difference on measurements was not quantified in this study.

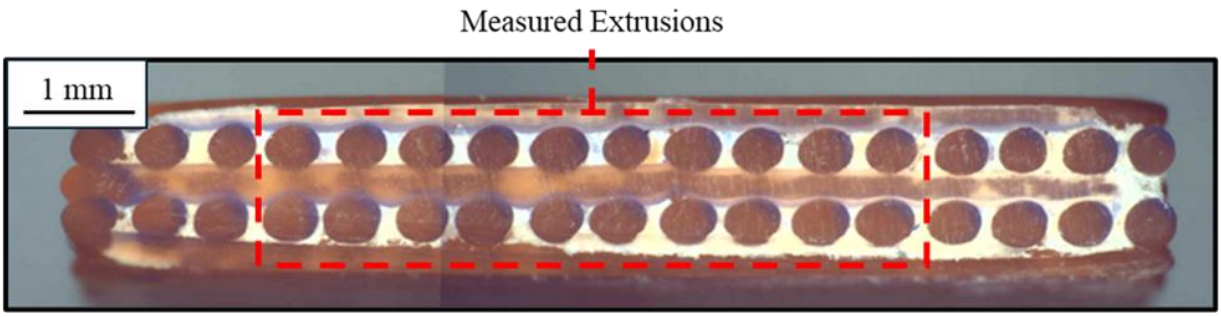

Figure 3 – Specimen used for measuring repeatability within a print with a 10% coating filament mix ratio and a 0.84 rev/mm rod rotation ratio. Extrusions 4 through 13 were measured on each layer, still avoiding the specimen edges because of deformation that occurs there.

Table 2 – Extrusion measurement deviation in a single specimen

	+X Extrusions			-X Extrusions			Averages of Directional Deviations	
	Layer 2	Layer 4	Whole Print	Layer 2	Layer 4	Whole Print	Layers 2 and 4	Whole Print
Data Points	5	5	10	5	5	10	20	20
Center Point Deviation (°)	0.152	0.492	0.344	0.212	0.277	0.241	0.283	0.293
Width Deviation (°)	0.396	0.901	0.665	1.200	1.004	1.046	0.875	0.856

Deviations for + or – X extrusions represent the variation of extrusions printed in the given direction, observed inside a single layer or through the whole print. Averages of directional deviations represent variation of center point and width from identical extrusions observed within the context of a single layer or the whole print.

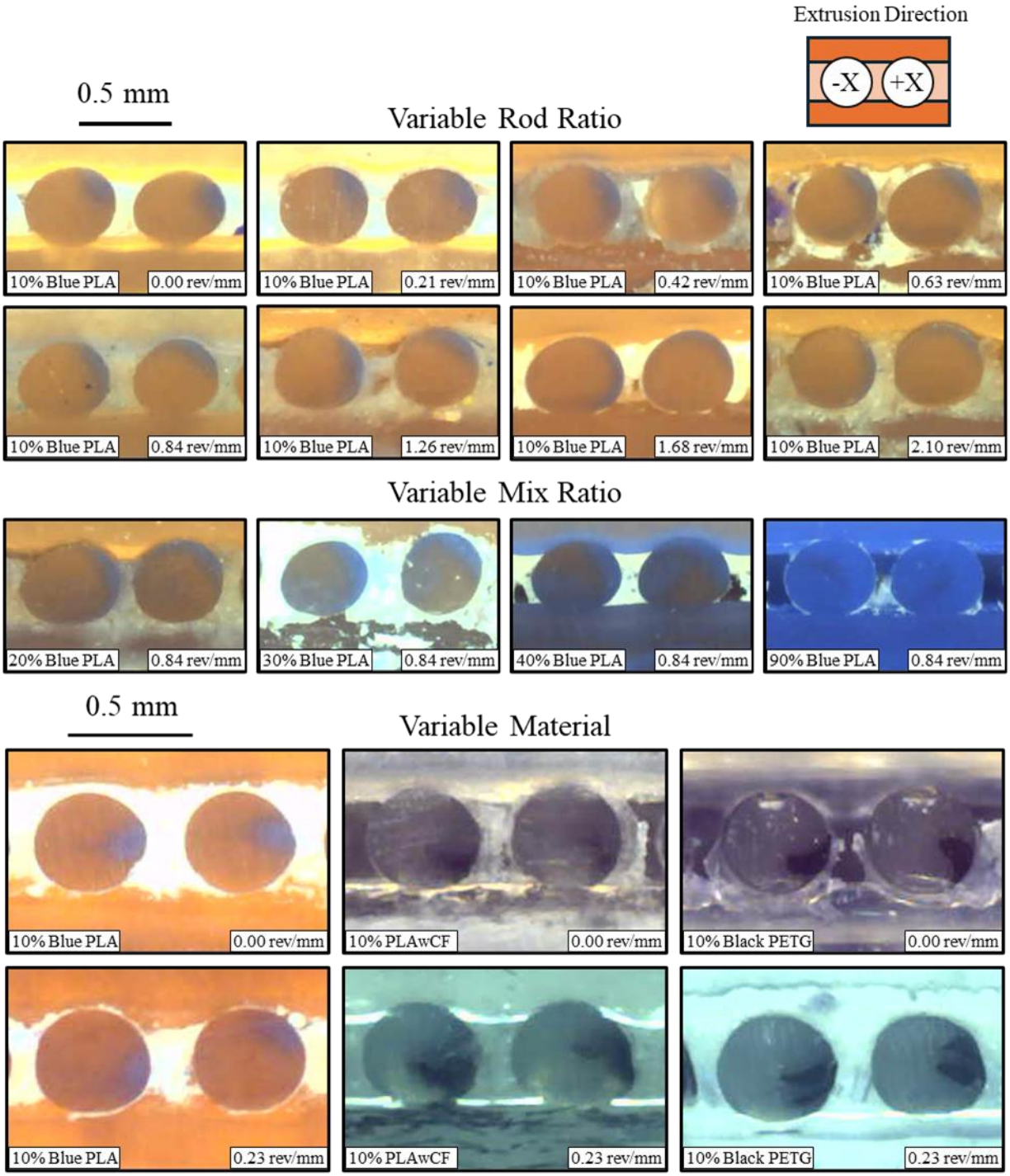

Figure 4 – Resulting print cross sections with a variety of print parameters. The 10% Blue PLA at 0.84 rev/mm specimen exists in both variable rod rotation and mix ratio data sets. Specimens varying rod and mix ratio only were printed in a hotend without composites, while those that compared the use of PLA with carbon fiber (PLAwCF) and PETG were printed on a second printer that has used composites before. Variability among printers was not investigated and results should only be compared between prints from the same origin.

Variable rod rotation

The data collected from the specimens with a 10% coating mix are presented at the left of Figure 5. Representative polar plots describe the coating size and location for each direction of extrusion, which is additionally plotted as a function of rod rotation. The measured widths of coatings did not change drastically as the rod spun more relative to the flow of filament, increasing from a minimum of 47.2° to a maximum 85.4° for the positive extrusions and from 52.5° to 84.1° for the extrusions traveling in the negative X direction. Neither of the maximums were recorded at the highest rod rotation ratio. Center points alternatively varied more, but the variation was not the same for both directions of printing. Extrusions printed in the positive X direction appear to have an increasing center point location until 0.84 rev/mm of rotation, after which the change in center point nearly flattens out. Extrusions oriented to -X have variation early on but appear to take on a linear trend as the rod rotation increases. The opposite response of the directions matches the expected behavior as the direction of printing changes external flow even if the flow through the hotend is consistent.

Variable filament mix ratio

The right side of Figure 5 presents the change in width and location caused by increasing the proportion of the coating material in the filament flow through the hotend. The change in center point of the coating does not linearly vary throughout the full range of the material ratios. Additionally, the width of the coating did not proportionally increase with the ratio. The circumference tends to have coating widths which cover a proportion greater than the filament mix ratio. As an example, half the circumference is covered at only a 40% ratio of coating per total extrusion. The width of the non-coating material, as estimated as 360° minus the coating width, is always smaller than the coating material. When present as the coating at a 10% ratio, the blue PLA has a coating width of 62.5°, while it coats 339° of the extrusion at a 90% ratio. This would indicate that the red PLA only coats 21° of the extrusion surface as a coating.

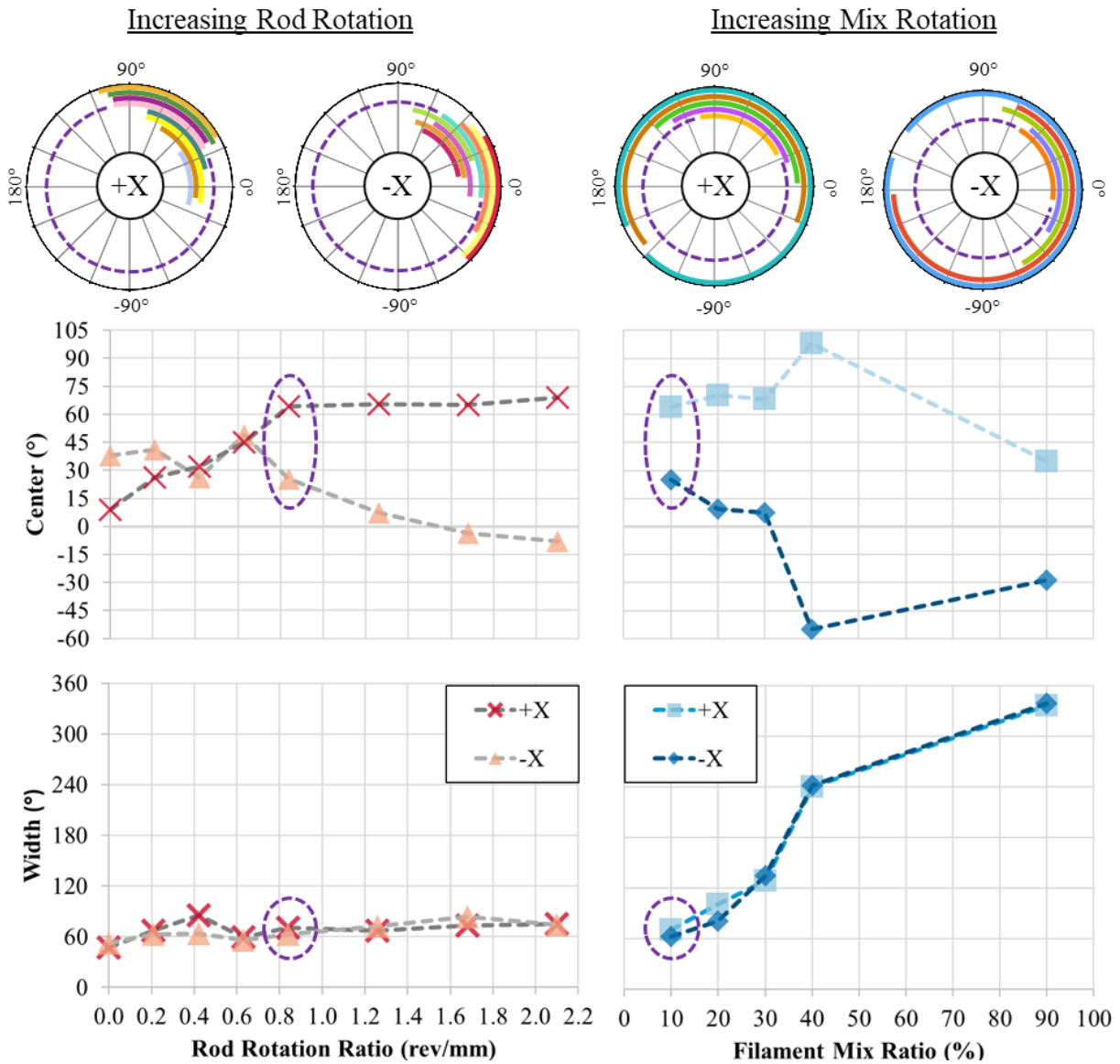

Figure 5 – Measured changes in coating center point location and width from adjusting the rod rotation and filament mix ratios. Specimens on the left were printed with a 10% filament mix ratio and rod velocities increasing from 0 to 2.1 rev/mm. Specimens on the right were printed with 0.84 rev/mm rod mixing and mix ratio increasing from 10% to 90%. Representative visuals for the + and – extrusion directions are given for each. The purple outlined data points and the purple line in the representative plots are a single specimen with a 10% filament mix ratio mixed with a rod ratio of 0.84 rev/mm.

Variation caused by material combinations

Measured coatings from specimens with chopped carbon fiber (PLAwCF) and PETG as the coating materials are presented in Figure 6. Material changes primarily resulted in shifts of the center point though changes in width were observed. Differences in results with changing material and other specimens is likely due using a different mixing hotend that has previously had composites in it. The differences caused by changing print direction aligns with the observed results of the other specimens at these rod and mix ratios. The PLA+PLAwCF and PLA+PETG in

Figure 6 appear less mixed than specimens that only changed pigment presented in Figure 5, which could be a result of changing composition or difficulties with imaging.

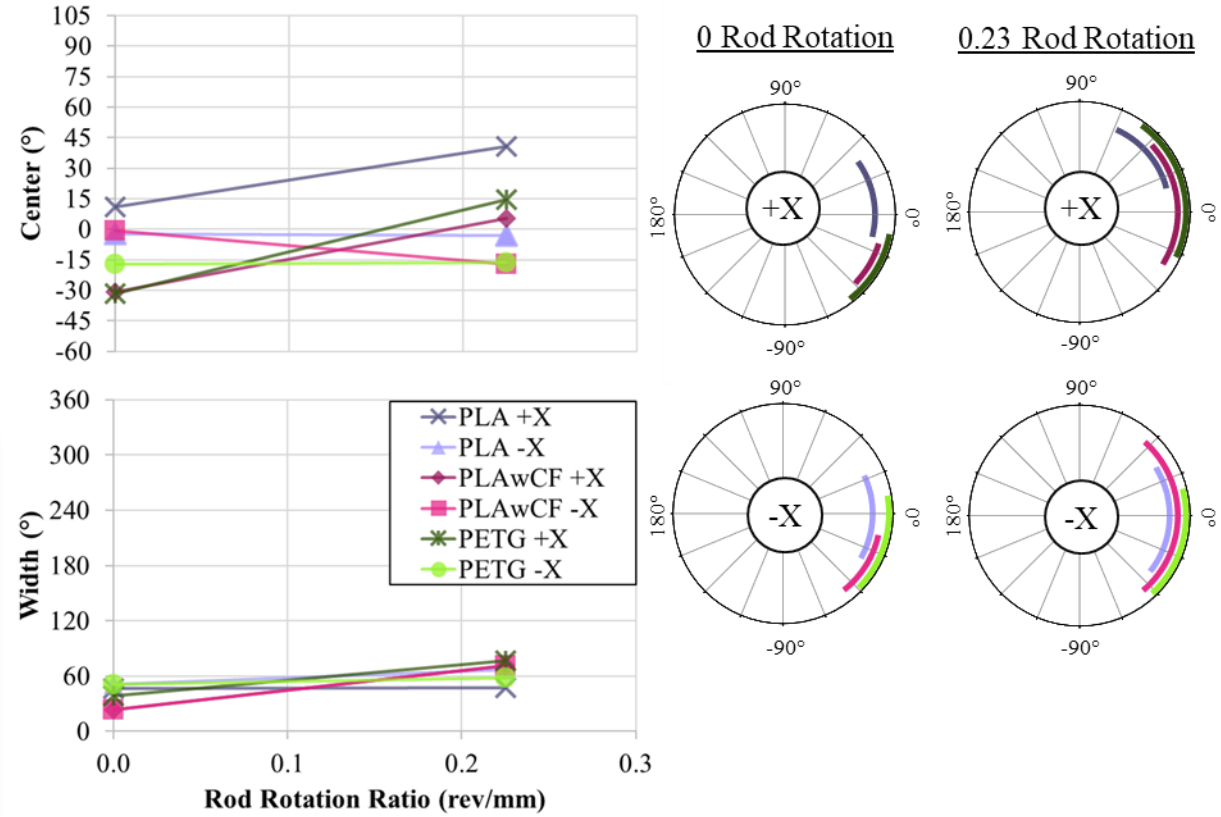

Figure 6 – Measured results from prints from the mixing printer using PLA with chopped carbon fiber (PLAwCF) and PETG as the coating materials. Pigmented PLA is used as a baseline for this printer's specific performance. As was observed with pigmented specimens, the coating center position is more affected than the width by increasing rod rotation ratio. The pigmented PLA is most dissimilar to the changed materials in center point location, especially in the +X direction.

Extrusion width and height

Though specimen heights and widths as instructed through print commands were always the same value, a preliminary observation was preformed to qualitatively observe the impact of extrusion geometry on the coating location. This print, shown in Figure 7 demonstrated that extrusion height and width, and the relationship between them, causes distortion of the extrusion coatings as it is deposited.

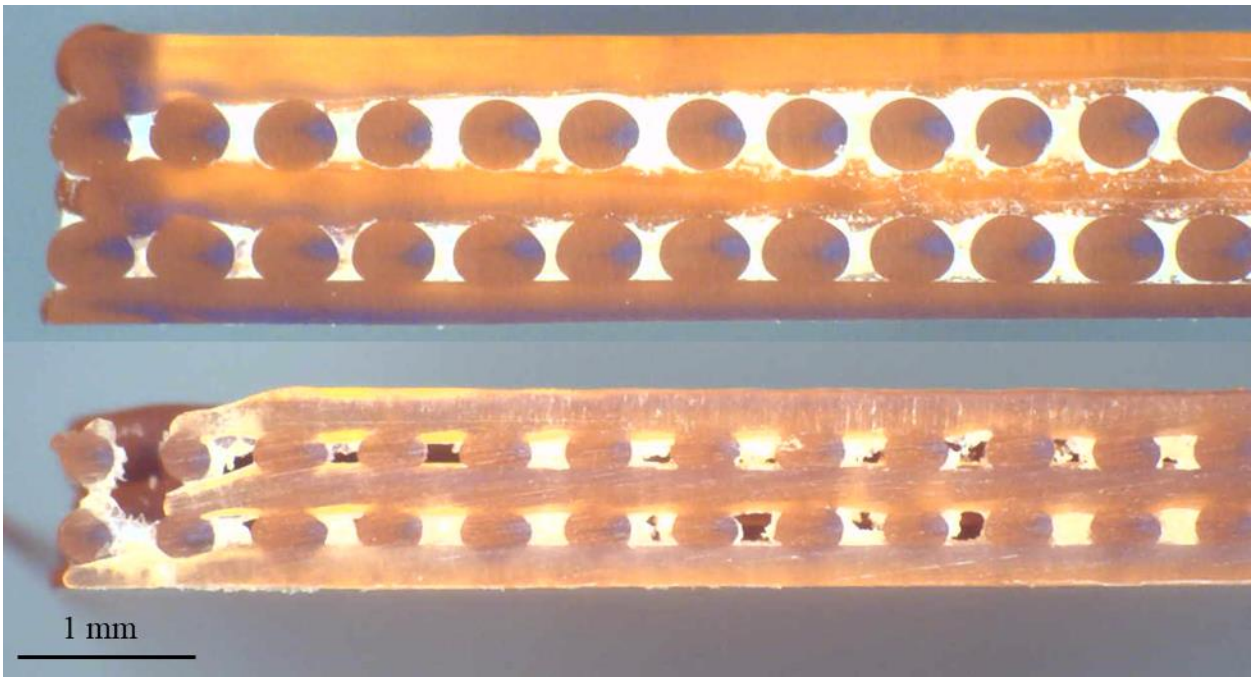

Figure 7 - Comparison of prints from the same printer with a 10% coating mixed at 0.84 rev/mm. Both specimens have 0.4 mm extrusion widths separated by 0.2 mm gaps. The top specimen has an extrusion height of 0.4 mm while the bottom specimen has a 0.2 mm extrusion height. All layers are affected by this change.

Impact of external flow processes

Across all specimens, a difference was observed between extrusions printed in the positive and negative X directions as this study did not fully investigate the impact of print directionality on coating behavior and only measured extrusions printed parallel to the X axis. The agreement of coating width measurements between directions indicates that external flow caused by direction of print primarily impacts center point location. The impact of other external parameters and print processes including non-uniform directions relative to the material inlets, print speed, neighboring extrusions, environment temperature, and bed temperature were kept constant through this study.

Discussion

Composition along the circumference of an extrusion's cross section during steady flow conditions is affected by rod rotation and filament mix ratios as indicated by the results presented in Figure 5. In effect, a combination of these settings may be assigned to coat a target region of an extrusion's circumference. Some range of composition assignment along the circumference while extruding in the +/- X direction can be achieved with a low filament mix ratio by altering the rod rotation as seen in Figure 1, but this method is limited at high ratios of rod rotation since the extrusion constituents mix and homogenize [2]. The combination of parameters for rod rotation, filament mix ratios, and print direction can facilitate composition assignment for a single target region of the perimeter without requiring the whole extrusion to change in composition. The relation between the range of the perimeter, $\gamma_{possible}$, that can be covered relative to a set maximum coating width, $\gamma_{coating}$, is presented in Figure 8 providing insight into the design space that was observed using the methods of this study. Capabilities may exist that produce a greater

circumference coating at a lower $\gamma_{coating}$. Print requirements for many applications will not be limited to extrusion along the +X and -X directions and are likely to operate with unsteady conditions such as variable print direction and flow rate indicating that more conditions should be characterized to further expand the design space to meet the needs of a wide variety of print applications.

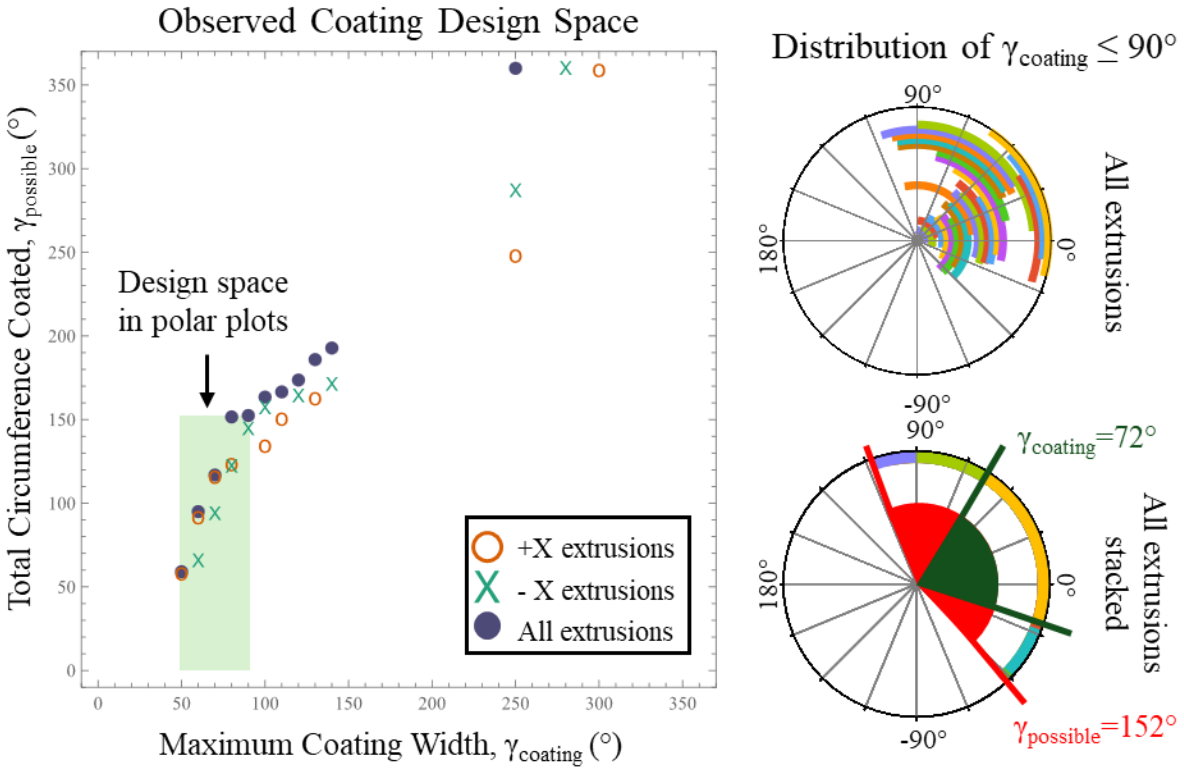

Figure 8 – Theoretical design space observed across all pigmented specimens from the same printer. The graph at the left plots the total combined extrusion circumference that was coated, $\gamma_{possible}$, against the maximum allowed width of any single coating, $\gamma_{coating}$. While both directions of extrusion are possible in a print, it may not always be favorable to use one or the other depending on toolpaths. The distribution of measured results with a $\gamma_{coating}$ less than or equal to 90° is presented in the polar plots at the right, first as each individual measurement and then their combined performance. These results are pulled from all specimens from the pigment only printer, at any combination of rod rotation ratio and coating mix ratio.

Ideal control would enable selective coverage across the full $\gamma_{possible}$ at near zero $\gamma_{coating}$ irrespective of print direction, flow rate, extrusion width, extrusion height, and unsteady conditions. Future work may demonstrate increased control without requiring any physical changes to the printer. Physical redesign to facilitate dynamic inlet position relative to the print direction may be necessary to achieve higher levels of control over the coating position, especially during unsteady print conditions. Interior surfaces of the hotend may also impact performance of the microstructure control by reducing or increasing the mixing of filaments in the melt chamber

Experimental results were derived using unidirectional rod rotation alone, indicating that increased composition control may be achieved by including bidirectional rod rotation. The specimens in this study with a filament mix ratio of 10% coating material, unidirectional rod rotation, printed in the -X direction, and a $\gamma_{coating}$ of 90° enabled a minimum total coating of circumferences of 145°. Bidirectional rotation can be expected to greatly increase the range of

composition control by shifting the center points in the opposite direction that they were shifted in this study, but will not double the range of control for $\gamma_{coating}$ as some of it is derived from the width of the extrusion and since the flow characteristics of the hotend may not be symmetrical. A lack of symmetry is expected because of physical features of the hotend like the off-center alignment of the inlets. Additionally, this design space may be further expanded by utilizing all three inlets, two for the coating material instead of one as was the case in this study. The active-mixing hotend inlets are positioned 120° apart which may reasonably be assumed to expand the design space proportionately. Future work utilizing more inlets and bidirectional rod rotation is expected to greatly increase the resolution of control and the commensurate design space.

Though the analysis and measurements emphasize composition control for coating the surface of extrusions, these results demonstrate capabilities for sub-extrusion composition control in FFF increasing the resolution beyond the dimensions of the extrusion itself. Using this technique, larger nozzles may be used to facilitate faster printing while maintaining the necessary resolution for composition control. This work also demonstrates an increase in versatility in FFF printing with an active-mixing hotend as it adds support for microstructural control within an extrusion at the same time supporting those techniques which can generate advanced features like functional gradients through LCC. Print planning to utilize these features may be facilitated through approximations based on the results of this work, but the effects of some major parameters were not explored and pose a challenge to accurate print planning throughout a complex print geometry. Notably, characterization is necessary to relate the effects of dynamically changing print direction, rod rotation, and filament mix ratio. A model to characterize flow through the hotend may be necessary to properly predict microstructures and inform selection of print parameters. Software should then be developed to automate dynamic control of the print instructions, including print parameters, toolpaths, and mixing control, to facilitate user design of coating widths and locations through a print.

This study limited the scope of the investigation by constraining many of the physical characteristics of the system such that the number of independent variables is manageable. Investigations should measure the impact of other properties of the printing system and the extrusions it produces. External factors such as existing print geometry, ambient temperature, and even bed surface may impact flow of coatings and sub-extrusion depositions after they leave the nozzle. Printer construction, including the hotend, rod, and nozzle surfaces and composition, could result in changes to the mixing characteristics. Material selection may also have great impact, as incompatible filaments may reduce mixing while promoting coating structures. Some composites may additionally present challenges as fibers and particulates may behave differently under turbulent, non-steady flow conditions and with additional effects from gravity. Extrusion properties, such as polymer phase blending, fiber distribution, and cross-sectional composition should be investigated through other methods beyond optical, including microCT when it can differentiate between the core and coating materials of the extrusion.

Future work should apply this technique to explore its use for manufacturing multifunctional and functionally graded materials as well as its use to improve FFF print performance. At the most basic level, this control reduces the amount of material purge necessary to produce an aesthetic coating when using similar materials, such as with a pigmented filament, and could reduce material waste and print time. Producing sub-extrusion scale support interfaces

using soluble or breakaway materials may create smoother part surfaces after post-processing. Additionally, controlled embedding of materials with a higher print temperature in extrusions of a lower temperature material may enable hotends to deposit materials even if the material's melt temperature is higher than the operational temperature of the hotend. Internal and external surfaces of prints may be coated with specific materials for benefits such as weight and cost reduction and corrosion resistance. Multifunctional materials, such as electrically conductive carbon black or ferromagnetic iron particles may be deposited into prints at a resolution smaller than the print nozzle, facilitating precise structure control and use of these material properties, such as creating electrical traces or specific magnetic fields within a print's substructure. Sub-extrusion depositions of soluble material may be removed through post-processing and produce lattice structures smaller than the size of extrusions, which can reduce print time and increase existing printer capabilities.

Conclusion

Local control of composition in additive manufacturing has great potential for improving properties and multifunctional characteristics of printed materials. Though the dimensional resolution of composition control in FFF is often limited to the geometry of a single extrusion, this study investigated the use of an active-mixing hotend to achieve microstructural control of compositions within extrusions. To investigate the controlled coating of singular extrusions, a combination of ranges of mixing rod rotation proportional to material flow and secondary material proportion of total extrusion were printed and investigated. Optical characterization of the extrusion cross-sections at steady state using colors to indicate the secondary material revealed that rod rotation has the greatest impact on the center point of the coating and the proportion of the coating material has the greatest impact on coating width. Extrusions with identical parameters show little deviation in coating properties and the combination of polymers and composites does not greatly impact coating behavior. Other variables were observed to affect the coatings but were not closely investigated in this study. These mechanisms for controlling microstructures have the potential to be controlled *in situ* through software, enabling fabrication of multifunctional materials and functional gradients with a wide variety of strength, stiffness, thermal and electrical conductivity, solubility, and corrosion resistance at a scale smaller than even the nozzle diameter.

Acknowledgements

The authors wish to thank the students from UTEP for their help with this study, including Viviana Morales, Karla Rodriguez, and Baldomero Fuentes for their assistance with specimen tuning and printing, post-processing procedures, and data collection.

Funding

The authors wish to acknowledge support from the UTEP Vice President of Student Affairs and Campus Office of Undergraduate Research Initiatives.

Conflict of Interest

The University of Texas System board of regents has patents for technologies described in this work for which Ian A. Rybak and Joshua T. Green are inventors.

References

[1] B.A. Moreno-Núñez, C.D. Treviño-Quintanilla, J. Carlos Espinoza-García, E. Uribe-Lam, E. Cuan-Urquizo, Effect of Printing Parameters on the Internal Geometry of Products Manufactured by Fused Filament Fabrication (FFF), (2023) 13–17.

[2] J.T. Green, I.A. Rybak, J.J. Slager, M. Lopez, Z. Chanoi, C.M. Stewart, R. V. Gonzalez, Local composition control using an active-mixing hotend in fused filament fabrication, Addit. Manuf. Lett. 7 (2023). https://doi.org/10.1016/j.addlet.2023.100177.

[3] J.T. Green, I.A. Rybak, C. Glaesman, Backup-Ring Optimization for High-Temperature and High-Pressure Applications Through Dynamic Composition Modification in Composite 3d Printing, Int. Pet. Technol. Conf. IPTC 2024. (2024). https://doi.org/10.2523/IPTC-23353-MS.

[4] Home | Marlin Firmware, (2018). https://marlinfw.org/ (accessed July 25, 2023).

[5] F. Lavecchia, M.G. Guerra, L.M. Galantucci, Chemical vapor treatment to improve surface finish of 3D printed polylactic acid (PLA) parts realized by fused filament fabrication, Prog. Addit. Manuf. 7 (2022) 65–75. https://doi.org/10.1007/s40964-021-00213-2.

[6] L.M. Galantucci, F. Lavecchia, G. Percoco, Experimental study aiming to enhance the surface finish of fused deposition modeled parts, CIRP Ann. - Manuf. Technol. 58 (2009) 189–192. https://doi.org/10.1016/j.cirp.2009.03.071.

[7] N.N. Kumbhar, A. V. Mulay, Post Processing Methods used to Improve Surface Finish of Products which are Manufactured by Additive Manufacturing Technologies: A Review, J. Inst. Eng. Ser. C. 99 (2018) 481–487. https://doi.org/10.1007/s40032-016-0340-z.

[8] P.M. Pandey, N.V. Reddy, S.G. Dhande, Improvement of surface finish by staircase machining in fused deposition modeling, J. Mater. Process. Technol. 132 (2003) 323–331. https://doi.org/10.1016/S0924-0136(02)00953-6.

[9] F. Lambiase, S. Genna, C. Leone, Laser finishing of 3D printed parts produced by material extrusion, Opt. Lasers Eng. 124 (2020) 105801. https://doi.org/10.1016/j.optlaseng.2019.105801.

[10] J. Žigon, M. Kariž, M. Pavlič, Surface finishing of 3d-printed polymers with selected coatings, Polymers (Basel). 12 (2020) 1–14. https://doi.org/10.3390/polym12122797.

[11] R.G. Lahaie, C.J. Hansen, D.O. Kazmer, Development of Fused Deposition Modeling of Multiple Materials (FD3M) Through Dynamic Coaxial Extrusion, Https://Home.Liebertpub.Com/3dp. (2023). https://doi.org/10.1089/3DP.2022.0197.

[12] Z.C. Kennedy, J.F. Christ, Printing polymer blends through in situ active mixing during fused filament fabrication, Addit. Manuf. 36 (2020) 101233. https://doi.org/10.1016/j.addma.2020.101233.

[13] Z. Liu, M.A. Meyers, Z. Zhang, R.O. Ritchie, Functional gradients and heterogeneities in biological materials: Design principles, functions, and bioinspired applications, Prog. Mater. Sci. 88 (2017) 467–498. https://doi.org/10.1016/j.pmatsci.2017.04.013.

[14] T. Teng, Y. Zhi, M. Akbarzadeh, Single-Nozzle Multi-Filament System with Active Mixing for High-Fidelity Multimaterial Additive Manufacturing, Addit. Manuf. (2024). https://ssrn.com/abstract=4773564.

[15] F. Daniel, A. Gleadall, A.D. Radadia, Influence of interface in electrical properties of 3D printed structures, Addit. Manuf. 46 (2021) 102206. https://doi.org/10.1016/j.addma.2021.102206.

[16] E. MacDonald, R. Wicker, Multiprocess 3D printing for increasing component functionality, Science (80-.). 353 (2016). https://doi.org/10.1126/science.aaf2093.

[17] I.M. El-Galy, B.I. Saleh, M.H. Ahmed, Functionally graded materials classifications and development trends from industrial point of view, SN Appl. Sci. 1 (2019) 1–23. https://doi.org/10.1007/s42452-019-1413-4.

[18] B. Saleh, J. Jiang, R. Fathi, T. Al-hababi, Q. Xu, L. Wang, D. Song, A. Ma, 30 Years of functionally graded materials: An overview of manufacturing methods, Applications and Future Challenges, Compos. Part B Eng. 201 (2020) 108376. https://doi.org/10.1016/j.compositesb.2020.108376.

[19] A. Creegan, P.M.F. Nielsen, M.H. Tawhai, A novel two-dimensional phantom for electrical impedance tomography using 3D printing, Sci. Rep. 14 (2024) 1–14. https://doi.org/10.1038/s41598-024-52696-y.

[20] A. Thakur, X. Dong, Additive manufacturing of 3D structural battery composites with coextrusion deposition of continuous carbon fibers, Manuf. Lett. 26 (2020) 42–47. https://doi.org/10.1016/j.mfglet.2020.09.007.